Prioritized Information Recovery for Wireless Link-Layer Communication

Sohraab Soltani and Hayder Radha
Department of Computer Science, University of Texas at Tyler, Email: soltanis@msu.edu
Department of Electrical & Computer Engineering, Michigan State University, Email: radha@egr.msu.edu

***Abstract*—In this paper we develop Prioritized Automatic Code Embedding (PACE) link-layer protocol to achieve preferred data recovery order across connections, while maintaining stable and reliable data flows over wireless networks. We classify link-layer traffic arrivals into different priorities based on the packet delay constraint and the distortion associated with the loss of that packet. The traffic arriving in each priority class is modeled as a poisson process. Consequently, we formulate the link-layer buffer as a multiclass M/G/1 priority queuing system where the decoding process (service process) of the PACE buffer is captured by a nonhomogeneous geometric distribution. This formulation enables the determination of an optimal dynamic decoding schedule for heterogeneous link-layer traffic arrivals. PACE employs a novel rate-adaptive Low Density Parity Check (LDPC) channel code for error recovery. We model the underlying LDPC decoding process and use it to determine an optimal code selection policy for maximal bandwidth utilization. We demonstrate experimentally that PACE reduces the throughput-delay cost by 20%-70% in comparison with the IEEE802.11 ARQ and Hybrid ARQ (HARQ) protocols. Further, the PACE protocol achieves 20%-60% improvement in channel bandwidth utilization and 2-10dB PSNR gain in realtime video quality.**

I. Introduction

To achieve superior link-layer wireless communication one need to target the following critical objectives: (i) achieving sustained traffic stability (maintaining continuous realtime flow under delay constraints), (ii) ensuring maximal reliability and throughput, (iii) exploiting side-information for channel estimation/prediction, and (iv) interacting with the higher layers for prioritized communication and improving quality of service. We believe that these objectives represent a viable and necessary set to support a diverse wireless link-layer communication with various requirements in rate, reliability, and delay. However, achieving these objectives simultaneously is a difficult task since they have conflicting requirements. In our prior work [1], we have demonstrated the feasibility of designing stable and reliable link-layer under Automatic Code Embedding (ACE) framework over point-to-point (single-hop) 802.11 channels. However, what is ultimately needed is a comprehensive framework that targets all of the above objectives (stable-and-reliable communications, exploitation of side information, and interaction with the higher layers) jointly.

In recent years, various decoding schedulers [2]–[4] have been proposed to improve the overall throughput in wireless link-layer communication. The majority of these efforts either consider the standard ARQ approach [5] or the Hybrid ARQ (HARQ) schemes [6] such as: diversity combining [7], code combining [8], and incremental redundancy. Approaches outlined in [6]–[8] are based on code puncturing methods [9]. These techniques assume (i) the complete knowledge of channel quality; and (ii) a slow-fading wireless environment. Under such assumptions, a decoder scheduling scheme only attempts to balance the quality of service for heterogeneous traffic requirements. This design strategy only targets quality of service and largely ignores the other objectives of wireless link-layer communication outlined above.

In this paper, we build on the ACE framework [1] to achieve preferred data recovery order across connections, while maintaining stable and reliable data flows in wireless networks. Under the proposed Prioritized ACE (PACE) framework, our ACE based stable-and-reliable[1] link-layer will employ a novel rate-adaptive Low Density Parity Check (LDPC) channel codes while interacting with the higher layers to provide a dynamic decoder scheduling service over varying wireless channel condition. Specifically, we develop a LDPC decoding model to capture the decoding process for link-layer traffic and use it to determine an optimal code selection strategy for maximal bandwidth utilization. Further, we find an optimal code embedding rate under the PACE framework to jointly meet the reliability, stability, and delay constraints of the wireless link-layer communication. We classify heterogeneous link-layer traffic arrivals into different priority classes based on packet delay constraints and the distortion suffered. The traffic arriving in each priority class is modeled as a poisson process. Consequently, we formulate the link-layer buffer as a multiclass $M/G/1$ priority queuing system where the decoding process (service process) of the PACE buffer is captured by nonhomogeneous geometric distribution [10]. Given the link-layer buffer model and the LDPC decoding model, we determine the optimal dynamic decoder scheduling under the PACE framework. This scheduling policy is a special

This paper is based on "On Link Layer Prioritization for Wireless Communication," by S. Soltani, K. Misra, and H. Radha, which appeared in the Proceedings of the 2oth International Conference on Computer Communication Networks (ICCCN), Maui, Hawaii, August 2011. © 2011 IEEE.

[1]For the definitions of reliability and stability under the ACE framework refer to [1].

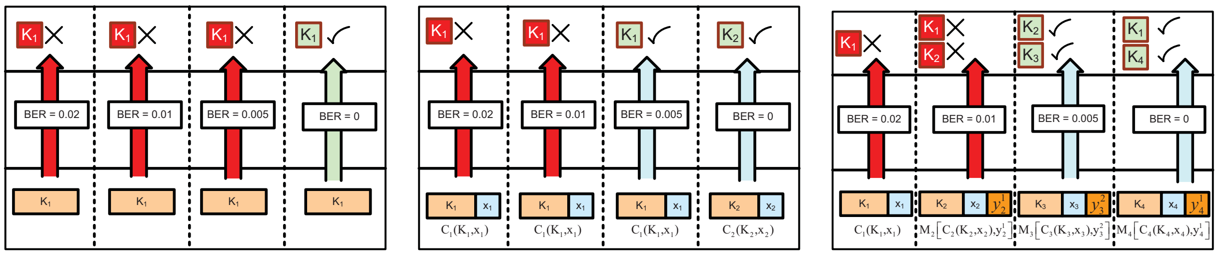

(a) IEEE802.11 ARQ (b) HARQ (c) PACE

Fig. 1. A wireless link-layer communication example consisting of four transmission intervals under different error control protocols.

case of a classic scheduling problem solved by Plambeck et al. in [13] and is asymptotically optimal.

The PACE protocol incorporates the LDPC model and the dynamic scheduling policy into the original ACE protocol [1]. We show experimentally that PACE improves the performance of the ACE protocol over wireless channels with varying conditions. Our contributions are:

- Develop a LDPC decoding model used to select the code with best error-correcting capability from an ensemble of codes.
- Model the link-layer buffer as $M/G/1$ priority multiclass queuing system to determine an optimal dynamic decoder scheduling policy to achieve improved quality of service while maintaining sustained stability.
- We develop the PACE protocol that provides reliable and stable wireless communication for high demand and delay sensitive heterogeneous link-layer traffic.

We present an extensive evaluation of our proposed link-layer protocol in comparison with the IEEE802.11 ARQ and HARQ protocols under varying channel conditions over real channel traces collected on 802.11b WLAN [1]. PACE is implemented using OMNET++ network simulator [19], and an Adaptive Low parity Density Code (A-LDPC) [18]. We begin by evaluating the impact of throughput-delay tradeoff on the performance of the PACE protocol. Empirical results show that PACE has the lowest throughput-delay cost in comparison with the IEEE802.11 ARQ and HARQ protocols. For instance, PACE reduces the cost by 20%-70% (over channels with bit error rate (BER) 0.018). Overall, the PACE protocol gains $10\% - 40\%$ reduction in throughput-delay cost over ACE. In addition, we measure the performances of a *realtime* video (using `H.264/AVC JM14.0` codec) [20] and a *non-realtime* TCP applications (using OMNET++ `INET framework`) in conjunction with PACE.

The remainder of the paper is organized as follows: In Section II, we give an example to demonstrate the efficacy of PACE in improving throughput-delay performance in wireless link-layer communication. The LDPC decoding and PACE receiver buffer models are derived in Section III. Section IV describes the PACE protocol. In Section V, we evaluate the performance of PACE. Section VI concludes the paper.

II. Illustrative Example

In this section, we briefly consider a communication example between two wireless nodes. This example consists of four transmission intervals where each transmission interval τ represents a time slot during which a sender transmits a packet and receives its acknowledgment. The sender wants to transmit four data packets (e.g., $K_1, \cdots, K_4$) each with length of k bits to the receiver. The first and the last packets (K_1 and K_4) are non-realtime. That is, impact of the delay in delivering these packets to a higher layer is insignificant on the performance of the corresponding application (e.g., SMTP packets). On the other hand, K_2 and K_3 are realtime. Consequently, these packets should be passed up to the higher layer within an end-to-end delay constraint, otherwise they are unusable for the application (e.g., realtime video packets). The wireless channel condition is gradually improving. Specifically, the channel is in severe condition (BER greater than 0.02) in τ_1. During τ_2 and τ_3 the channel BER reduces to 0.01 and 0.005 and finally the channel is error-free in τ_4. We consider the following scenarios:

1) *Ideal scenario:* Under an ideal scenario all four packets are transmitted over the channel and received without errors. This gives the throughput of one and all packets are delivered to the higher layer. However, since the channel BER is non-zero in the first three transmission intervals, the odds of receiving an error-free packet are very low.
2) *IEEE802.11 ARQ:* This scheme uses a retransmission for error recovery. As illustrated in Fig 1(a), in τ_1, the sender transmits K_1. Since the channel BER is non-zero, the received packet is erroneous. Consequently, the receiver requests for a retransmission of K_1 in τ_2 and also in τ_3 because the channel BER is still non-zero. In τ_4, K_1 is finally delivered to the receiver without errors and passed up to the higher layer. This creates the throughput of $1 - \frac{3k}{4k} = 0.25$ since K_2, K_3 and K_4 are not transmitted during the four time-slot window of this simple example.
3) *Hybrid ARQ (HARQ):* Fig 1(b) shows the performance of HARQ. In τ_1, the sender encodes K_1 data packets with x_1 parity bits and creates a codeword $C_1(K_1, x_1)$. The receiver fails to decode C_1 and requests for a retransmission of C_1. In τ_2, the sender retransmits C_1. Since the channel BER is relatively

high (BER is 0.01), the receiver cannot decode C_1 and requests for the second copy of C_1. In τ_3, the receiver successfully decodes C_1. Consequently, in τ_4, the sender transmits $C_2(K_2, x_2)$. The channel is error-free in τ_4 and so the receiver decodes C_2 successfully. Data packets K_1 and K_2 are delivered to the higher layer. This creates the throughput of $0.25 \leq 1 - \frac{2k+x_1+x_2}{4k} \leq 0.5$ since K_3 and K_4 are not transmitted and furthermore, some of the channel bandwidth is consumed for the delivery of parity bits x_1 and x_2. Notice that in practice, the number of parity bits is significantly less than the number of data bits in a codeword (i.e., $x_i \ll k$).

4) *PACE:* Fig.1(c) shows the PACE protocol performance. In τ_1, a codeword $C_1(K_1, x_1)$ is sent. A receiver that fails to decode C_1, stores C_1 in its buffer and requests for additional parity bits (hereafter type-II parity bits) for C_1. In τ_2, the transmitter sends $M_2 = [C_2(K_2, x_2), y_2^1]$. The receiver uses x_2 to decode C_2 and employs type-II parity bits y_2^1 (y_i^j denote additional parity for $C_j, j < i$ transmitted in τ_i) in addition to x_1 to decode C_1. The receiver fails to decode C_1 and C_2. Since the codeword C_2 corresponds to the realtime data packet K_2, it has higher priority than C_1. Therefore, the receiver requests for type-II parity bits for C_2 rather than C_1. As a result, in τ_3, the sender transmits $M_3 = [C_3(k_3, x_3), y_3^2]$. In τ_3, the receiver successfully decodes C_3 using x_3 and $C_2(k_2, x_2 + y_3^2)$. Consequently, the receiver requests for type-II parity bits for C_1. Accordingly, in τ_4, the sender transmits $M_4 = [C_4(K_4, x_4), y_4^1]$. The receiver decodes C_4 using x_4 and $C_1 = (K_1, x_2 + y_2^1 + y_4^1)$ successfully. Therefore, the data packets $K_1, \cdots, K_4$ are delivered to the higher layer. The throughput under PACE is $0.75 \leq 1 - \frac{\sum_{i=1}^{4} x_i + y_2^1 + y_3^2 + y_4^1}{4k} \leq 1$.

This example demonstrates the efficacy of PACE in improving throughput-delay performance in wireless link-layer communication. However, the description above has intentionally ignored important details. For PACE to become practical we need to address the following challenges:

- *Optimal Parity Allocation:* PACE uses channel codes for error recovery and hence it requires embedding parity bits in every packet. Since the transmission of parity bits consumes channel bandwidth, it is important to identify the optimal allocation of parity bits in every transmission based on the channel condition and the channel code algorithm. A practical design of parity allocation for PACE has to ensure (i) high likelihood of successful decoding; and (ii) efficient utilization of the channel bandwidth.
- *Dynamic Decoder Scheduling* In every transmission, PACE should perform error recovery on the packets with higher priority and hence buffer less significant ones for future recovery. To achieve compliance with such policy, it is natural to consider two complementary modes of dynamic scheduling: (i) PACE should choose the order in which arriving packets are served to guarantee the delivery of the packets to the higher layer before they expired; and (ii) to reject or drop insignificant packets when the buffer length is judged to be excessive, thereby incurring penalties or lost potential throughput.

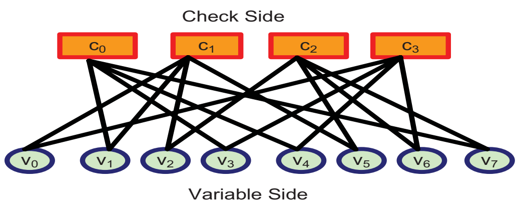

Fig. 2. A LDPC Tanner graph with $d_v = 2$ and $d_c = 4$.

The rest of the paper shows how to address these two challenges. To that end, in the next section, we study the behavior of the link-layer traffic under the PACE framework and formulate necessary models which provide essential tools to develop a practical design of PACE.

III. Model Formulation

In this section, we develop the following models for PACE: (i) *LDPC decoding model* which captures the decoding process of link-layer traffic using LDPC codes; (ii) *Buffer model* which describes the link-layer buffer as a multiclass priority queuing system with a single server. These models will build the framework to determine optimal code selection and dynamic decoder scheduling strategies for the PACE protocol.

A. LDPC Decoding Model

PACE employs LDPC codes for decoding link-layer packets. Our objective in this section is to formulate the LDPC decoding process to select the code with best error correcting capability to maximize bandwidth utilization. PACE uses the LDPC check matrix represented by Tanner bipartite graph shown in Fig 2. The nodes of the graph are separated into two distinctive sets which are called variable and check nodes with the degree of d_v and d_c respectively. The PACE protocol uses an iterative belief propagation LDPC decoder [12] which attempts to correct errors in the received packet in m iterations. The following equation, by Gallager [11] shows the reduction of errors as the function of the iteration number m:

$$\begin{aligned}\epsilon^{(m)} = \epsilon^{(0)} - \epsilon^{(0)} \left[\frac{1 + (1 - 2\epsilon^{(m-1)})^{d_c - 1}}{2}\right]^{d_v - 1} \\ + (1 - \epsilon^{(0)}) \left[\frac{1 - (1 - 2\epsilon^{(m-1)})^{d_c - 1}}{2}\right]^{d_v - 1},\end{aligned} \tag{1}$$

where $\epsilon^{(0)}$ represents the cross-over probability of the Binary Symmetric Channel (BSC) that the packet is transmitted over and $\epsilon^{(m)}$ is the probability of error in the packet after the m^{th} iteration.

Using Equation (1), we can formulate a relationship between the number of iterations in belief propagation method m, LDPC parity check matrix parameters d_v and

d_c, and the amount of error in the received packet. This relationship is communicated to us by Karande [14] and presented in the following Lemma:

Lemma 1. *For a packet transmitted over BSC with cross-over probability ϵ_i that is decoded using LDPC check matrix with parameters d_v and d_c; the distortion level after m iterations can be approximated by*

$$\epsilon_i^{(m)} \approx \epsilon_i \left[\epsilon_i(d_v - 1)(d_c - 1)\right]^{m-1}$$

Proof: See Appendix. ∎

In a transmission interval τ_i, the PACE sender creates a codeword $C_i(k_i, x_i)$ by employing LDPC generator matrix, thus encoding k_i data bits with x_i type-I parity bits. Correspondingly, the receiver attempts to retrieve k_i data bits by utilizing x_i parity bits embedded in the received packet C_i. Specifically, the receiver utilizes a LDPC check matrix with $n_i = k_i + x_i$ variable nodes and x_i check nodes. Since the degree of each variable and check node is d_v and d_c respectively, the following equality holds:

$$n_i d_v = x_i d_c. \tag{2}$$

Lemma 1 suggests that LDPC belief propagation performance depends on the knowledge of channel condition ϵ_i and the check matrix parameters d_v and d_c. In addition, the receiver can correct a certain level of error proportional to the number of parity bits embedded in the packet. Therefore, the receiver is capable of correcting up to $\alpha(\epsilon_i) \times x_i$ errors out of n_i bits in the packet. Here $\alpha(\epsilon)$ measures the expected error-correcting capability of the LDPC soft decision decoder when the channel BER is ϵ. The sender uses the channel n_i times to transmit a codeword $C_i(k_i, x_i)$. Consequently, the amount of error introduced in the received codeword (on average) is $\epsilon_i n_i$. As a result the receiver fails to decode $C_i(k_i, x_i)$ if the amount of error in the received packet exceeds the error correcting capability of the receiver. That is,

$$\epsilon_i n_i \geq \alpha(\epsilon_i) x_i. \tag{3}$$

Using Equations (2) and (3), we obtain an upper bound on $\alpha(\epsilon_i)$:

$$\alpha(\epsilon_i) \leq \epsilon_i \frac{d_c}{dv}. \tag{4}$$

Our main objective in this section is to select the code with best error-correcting capability. Toward this end, we employ Lemma 1 and Equation (4) to obtain the maximum value of $\alpha(\epsilon_i)$. According to Lemma 1, LDPC decoder successfully decodes $C_i(k_i, x_i)$ when the distortion level of the received packet after m iterations approaches zero. In practice, the LDPC belief propagation algorithm is configured such that the number of iterations m and the degree of variable nodes d_v are predefined and constant [18]. However, the degree of check nodes d_c is determined by the algorithm based on the number of available parity bits. Consequently, a successful decoding depends directly on d_c. On the other hand, Equation (4) suggests that error-correcting capability of the decoder cannot exceed the upper bound $\alpha_u(\epsilon) = \epsilon_i \frac{d_c}{dv}$. So, to maximize $\alpha_u(\epsilon_i)$, we have the following optimization problem:

$$\begin{gathered} \arg\max_{d_c} \alpha_u(\epsilon_i) \quad \text{subject to:} \\ \epsilon_i \left[\epsilon_i(d_v - 1)(d_c - 1)\right]^{m-1} \approx 0 \ \text{ and} \end{gathered} \tag{5}$$

Solving (5) leads us to the best possible value of d_c and the maximum error-correcting capability $\alpha^*(\epsilon_i)$. Consequently, we select a code from an ensemble of codes which has the error-correcting capability close to $\alpha^*(\epsilon_i)$. In Section IV, we will use this code to obtain the optimal parity allocation strategy for PACE.

B. PACE Buffer Model

Each arriving packet at the PACE receiver was generated to serve a specific protocol or application in the higher layers. Depending on the type of the protocol or application, the packet is confined to a specific delay constraint. In addition, the packet contains a certain level of distortion due to the impact of wireless link-layer transmission. Under the PACE framework, each packet is classified into a specific priority class based on its delay constraint and distortion. The PACE receiver then attempts to serve a specific priority class according to dynamic decoder scheduling rules. In Section IV-B we will provide a thorough description of packet prioritization process and dynamic decoder scheduling policy. These procedures require a complete formulation of the PACE buffer. Therefore, in this section, we develop a comprehensive queuing model for the PACE buffer. To that end, we first model the arrival process and the service distribution of each priority class.

Arrival Process and Service Distribution: We consider the Markovian channel introduced in [1]. The link-layer wireless channel is modeled as a discrete Markov chain with N states $S_1, \cdots, S_N$. Each state S_i is a representation of a BSC with a particular BER ϵ_i which is valued from a finite set F_N with length N: $\epsilon_i \in F_N, |F_N| = N$. In [1], and specifically Equation (4), we measured the probability of successful decoding of a packet $C(k_i, x_i)$ transmitted over the channel in state S_i. Using the LDPC decoding model, we reformulate this probability measure as follows:

$$P(E_i \leq \alpha(\epsilon_i) \times x_i) = F_{E_i}(\alpha(\epsilon_i) x_i) = \sum_{d=0}^{\lfloor \alpha(\epsilon_i) x_i \rfloor} e^{-\lambda_{E_i}} \frac{\lambda_{E_i}^d}{(d)!}. \tag{6}$$

Here E_i represents the packet distortion level that has a Poisson distribution with cumulative density function $F_{E_i}(u)$ and rate λ_{E_i}.

The PACE receiver stores the arriving packets in its buffer when the decodings with type-I parity bits are unsuccessful. Consequently, the arrival process of packets with distortion level E_i in the PACE buffer can be modeled as a poisson process with the rate λ_i which is equivalent to the probability of decoding failure with type-I parity bits:

$$\lambda_i = 1 - F_{E_i}(\alpha(\epsilon_i) x_i) = \bar{F}_{E_i}(\alpha(\epsilon_i) x_i). \tag{7}$$

On the other hand, each arriving packet at the PACE is confined to a specific delay constraint which is *independent* of the packet error. Consider the situation where a packet with delay constraints d_j arrives according to a Poisson process with rate λ_j. Notice that from the PACE buffer vantage point, the arrival process of this packet is *independent* of the arrival process of a packet with error E_i. However, both of these processes are Poisson processes. Therefore, if a packet with delay constraint d_j and distortion level E_i is classified into priority class l, then the arrival process of this priority class is a poisson process with rate λ_l where

$$\lambda_l = \lambda_i + \lambda_j. \tag{8}$$

A packet departs the PACE buffer either if (i) it is successfully decoded with additional type-II parity bits. In this case the data bits embedded in the packet are delivered to the higher layer; or (ii) its delay constraint expires, meaning that the packet is timed out and is dropped from the buffer. In the latter case the service distribution of the PACE decoder has zero density since the packet is dropped. In the former case, the service distribution depends on the probability of successful decoding of a packet with type-II parity bits. The probability of successful recovery of a particular packet increases as more type-II parity bits are added to the packet. Consequently, the error correction process of every packet under PACE has a nonhomogeneous geometric distribution [10] with the density function $f_G^i(t)$ with the parameter $p_t^i = F_{E_i}(\alpha(\epsilon_i)z_t)$:

$$f_G^i(t) = P(\text{Successful recovery on } t \text{ trial}) = p_t^i \prod_{k=1}^{t-1}(1-p_k^i). \tag{9}$$

where p_t^i measures the likelihood of successful decoding (when the channel is in state S_i) on t^{th} decoding trial using total parity bits (type-I and type-II) of z_t. Therefore, the service distribution G_l for a priority class l is $f_G^l(t)$ which is a truncated $f_G^i(t)$ on d_j:

$$f_G^l(t) = \begin{cases} f_G^i(t) & \text{if } d_j - t > 0 \\ 0 & \text{otherwise} \end{cases} \tag{10}$$

The service rate of priority class l is the expected value of the density function $f_G^l(t)$. That is,

$$\mu_l = E[f_G^l(t)] = \begin{cases} \frac{1}{p_t^i} & \text{if } d_j - t > 0 \\ 0 & \text{otherwise} \end{cases} \tag{11}$$

According to Equation (8), the traffic arriving in each priority class is a poisson process. On the other hand, a decoding process of each priority class has a nonhomogeneous geometric distribution given in (10). Consequently, the PACE buffer can be modeled with a multiclass $M/G/1$ priority queuing system with a single server. Here the arriving customers represent packets with different priority classes and the PACE decoder is the server.

Consider the situation where the packets in the PACE buffer are classified into $1, \cdots, L$ priority classes, which arrive according to independent Poisson processes with respective rates $[\lambda_l]_{l=1}^L$ and have service distributions $[G_l]_{l=1}^L$ as calculated in Equations (8) and (10). Let W_l denote *priority delay*, the average waiting time of a packet with priority class l in the PACE buffer before it is successfully transmitted to the higher layer. Our objective is to compute the W_l.

Under $M/G/1$ priority queuing system, V_l the average amount of decoding time for priority class l is as follows [15]:

$$V_l = \lambda_l E[G_l] W_l + \frac{1}{2}\lambda_l E[G_l^2]. \quad l = 1, \cdots, L \tag{12}$$

On the other hand, the *priority delay* of an arbitrary class l is equivalent to the amount of decoding time in the system requires upon its arrival plus the decoding time that remains for other arrivals classes that are already under the service. Therefore,

$$W_l = V_l + V_j. \quad j \neq l, l, j = 1, \cdots, L \tag{13}$$

Using Equations (12),(13) and some mathematical manipulations, we can solve for individual W_l:

$$W_l = \frac{\sum_{l=1}^{L} \lambda_l E[G_l^2]}{2\prod_{j=l-1}^{l}\left[1 - \sum_{k=1}^{j}\lambda_j E[G_j]\right]}. \tag{14}$$

In this section, we modeled the PACE buffer as a multiclass $M/G.1$ priority queuing system and we obtained the arrival and service rates, and the expected delay for each priority class in the buffer. In Section IV-B, we will employ this model to find an optimal dynamic decoder scheduling policy for PACE.

IV. PACE Protocol

In this section, we describe the design architecture of the PACE protocol and the functionality of each of its components. Fig 3 illustrates the architecture of PACE sender and receiver. PACE is built on the ACE framework developed in [1]. Specifically, in Fig. 3, the dark-colored components in sender and receiver sides are those components that are either added or modified in the PACE framework. In the following sections, we present a thorough description for these components.

A. PACE Sender

As illustrated in Fig. 3(a), the PACE sender has two components. The first component is *Channel State Prediction* where the link-layer wireless channel condition for the next transmission interval is predicted based on the receiver feedback. Specifically, the sender uses $\hat{\delta}_{i-1}$, the receiver channel estimate for τ_{i-1} as its prediction of the channel BER in current transmission interval τ_i; so $\hat{\epsilon}_i = \hat{\delta}_{i-1}$.

The second component is *Parity Allocation* where a new codeword is generated and an appropriate number of type-II parity bits is added to a packet for the next transmission. We use the LDPC model developed in Section III-A to select an appropriate code (based on the channel condition) to find an optimal parity allocation.

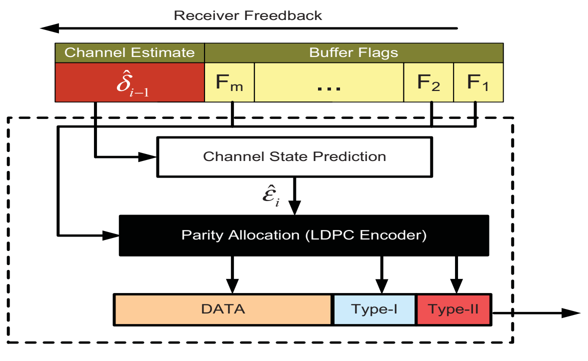

(a) PACE Sender

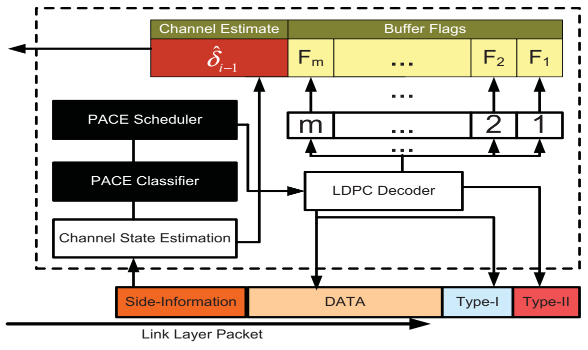

(b) PACE Receiver

Fig. 3. The design architecture of the PACE protocol.

In [1], we proved that under the ACE framework, there exist only one optimal code embedding rate under which the reliability and stability of link-layer traffic is ensured. Recall that the operational code embedding rate measures the fraction of data bits that are embedded in a codeword. For instance a codeword $C_i(k_i, x_i)$ is generated based on the code rate $R_i = \frac{k_i}{k_i+x_i}$. This finding is repeated in the following Lemma:

Lemma 2. *An optimal solution for code embedding rate that ensures reliability and stability in wireless transmission over a channel in state S_i is a unique solution and is given by:*

$$R_i = 1 - \frac{\epsilon_i}{\alpha}. \quad \epsilon_i \ll \alpha$$

where α is error-correcting capability of a decoder.

Proof: See Appendix. ■

Lemma 2 determines the optimal code embedding rate for a general decoder with error-correcting capability α. However, the LDPC decoder model selects a code (when the channel BER is ϵ_i) with a error-correcting capability close to $\alpha^*(\epsilon_i)$ computed in (5). In practice, PACE uses $\alpha^*(\hat{\epsilon}_i)$ to measure the expected error-correcting capability of the LDPC soft decision. This is so since PACE sender uses $\hat{\epsilon}_i$ as an estimate of the expected error in the next transmission interval τ_i. Therefore, an operational optimal code embedding rate for parity allocation is

$$R_i^* = 1 - \frac{\hat{\epsilon}_i}{\alpha^*(\hat{\epsilon}_i)}. \tag{15}$$

PACE first determines the amount of type-II parity bits (y_i^k) for a particular codeword C_k transmitted in some $\tau_k, k < i$. According to Equation (15) C_k with length n_k requires at most $z_i^k = \frac{n_k \hat{\epsilon}_i}{\alpha^*(\hat{\epsilon}_i)}$ parity bits for error recovery. However, for C_k, $x_k + \sum_{l=k+1}^{i-1} y_l^k$ parity bits are already transmitted in the previous transmission intervals $\tau_k, \cdots, \tau_{i-1}$. Thus, type-II parity bits necessary to transmit in τ_i for C_k is $y_i^k = z_i^k - x_k + \sum_{l=k+1}^{i-1} y_l^k$.

After allocating type-II parity bits for codewords in the PACE buffer, PACE has $n_i = n - \sum_k y_i^k$ bits to transmit a new codeword $C_i(k_i, x_i)$ where n is the maximum number of bits that can be transmitted in a packet. Similarly, the amount of parity bits necessary for encoding C_i is $x_i = \frac{n_i \hat{\epsilon}_i}{\alpha^*(\hat{\epsilon}_i)}$, and therefore the amount of *new* data in C_i is $k_i = n_i - x_i$. The PACE sender then transmits a new codeword along with the additional type-II parity bits in a new link-layer packet denoted by $M_i = [C_i(k_i, x_i), \mathbf{y}_i]$ to the receiver.

B. PACE Receiver

Upon the reception of the link-layer packet $M_i = [C_i(k_i, x_i), \mathbf{y}_i]$, the type-II parity bits are extracted and sent to the receiver buffer. PACE receiver first attempts to decode a codeword $C_i(k_i, x_i)$ with type-I parity bits x_i. If the decoding is successful, the data bits k_i are sent to the higher layer. But if the decoding fails, then the codeword is sent to the receiver buffer for future recovery.

Under the PACE framework, each packet is mapped to a specific priority class based on its delay constraint and distortion suffered. The PACE receiver then attempts to serve packets with a specific priority class according to dynamic decoder scheduling rules. The *Classifier* and *Scheduler* components in Fig. 3(b) implement the packet prioritization and dynamic decoder scheduling policy in the PACE receiver.

1) PACE Classifier: Consider a codeword $C_i(k_i, x_i)$ was transmitted over the channel with state S_i. Let d_j represent the delay constraint of the packet with the distortion level E_i. The PACE *Classifier* assigns this packet to a priority class l based on the parameters d_j and E_i using a classification function $g : [i, j] \to l$, where

$$g = g\left(h_D(\tau_i, d_j), f_G^i(\tau_i)\right) \quad i \in R^N \times j \in R^M : l \in R^{M\times N} \tag{16}$$

where $h_D(.,.)$ is the delay penalty function, and $f_G^i(t)$ is the error-correcting density function given in Equation (9). The domains of packet distortion and delay constraint values are presented by R^N and R^M respectively.

The delay penalty function $h_D(\tau_i, d_j)$ measures the cost of postponing the delivery of data bits k_i to the higher layer in transmission interval τ_i based on packet delay constraint d_j. Specifically, $h_D(.,.)$ ranges from zero to one where the cost of dropping a packet is one (the packet is never delivered). We use the following delay penalty function [16]:

$$h_D(\tau_i, d_j) = a \exp\left[b(\tau_i - d_j)\right], \tag{17}$$

where a and b are normalizing coefficients.

The PACE *Classifier* first computes the penalty weight for each packet stored in the PACE buffer. Specifically, the penalty weight w_l for a packet with distortion level E_i and delay constraint d_j is

$$w_l = h_D(\tau_i, d_j)\left[1 - f_G^i(\tau_i)\right]. \quad (18)$$

Notice that w_l approaches one if and only if the delay penalty function $h_D(.,.)$ reaches one and $f_G^i(.)$ is very small. This is an indication of a critical situation where the packet is reaching its deadline and has to be decoded immediately and at the same time the likelihood of decoding the packet with the current number of parity bits is very low. Therefore, the PACE *Classifier* classifies a packet with the highest penalty weight to a higher priority class. That is the priority classes $1, \cdots, L$ are numbered so that

$$w_1 \geq w_2 \geq \cdots \geq w_L.$$

2) PACE Scheduler: Accordingly to the PACE buffer model, the l^{th} priority class has the arrival rate λ_l, service rate μ_l, and the *priority delay* W_l, as obtained in Equations (8), (11) and (14). Consider a deterministic fluid analogy in which fluid of class l arrives at a constant rate λ_l and can be drained at rate μ_l if the PACE receiver devotes all its capacity to class l. If the fluid level of class l in the buffer is $N_l(t)$ at time t, then the oldest fluid of that class arrived $\frac{N_l(t)}{\lambda_l}$ time units earlier. Thus the fluid level of class l is not increasing if

$$\frac{N_l(t)}{\lambda_l} \leq W_l \rightarrow N_l(t) \leq \lambda_l W_l. \quad (19)$$

Therefore, the *backlog* of class l in the system at time t is given by:

$$\eta_l(t) = \frac{N_l(t)}{\lambda_l W_l} \quad (20)$$

Consequently, for a workload process $Q(t)$ defined as

$$Q(t) = \sum_{l=1}^{L} \mu_l N_l(t), \quad (21)$$

the associated threshold level is

$$q = \sum_{l=1}^{L} \mu_l \lambda_l W_l. \quad (22)$$

The PACE *Scheduler* performs the *dynamic decoder scheduling policy* which has two parts: (i) *Sequencing rule*: the PACE receiver at each decision point t (every transmission interval), decodes the oldest packet from the class l having the largest backlog $\eta(t)$; and (ii) *Rejection rule*: The PACE receiver drops a packet of class L (class L has the lowest priority significance) from its buffer if and only if $Q(t) > q$. Plambeck et al. in [13] proved that the above scheduling policy is asymptotically optimal under the heavy traffic condition.

In this section, we described the functionality of the *Classifier* and *Scheduler* components added in the PACE receiver. In the next section, we conduct extensive performance evaluations of PACE to demonstrate the advantage of the new components added to ACE in comparison with the original ACE protocol and other leading link-layer protocols.

V. Experiment

In this section, we present performance evaluations of the PACE protocol on real wireless channel traces collected on an 802.11b WLAN [1]. Specifically, we use 41 channel traces, each with unique average BER to simulate 41 various channel conditions. We compare the performance of the PACE protocol as opposed to the ACE, HARQ, and IEEE802.11 ARQ protocols. In particular, we first show the impact of throughput-delay tradeoff on the performance of each protocol. Then, we measure the performances of a *realtime* video and a *non-realtime* TCP applications in conjunction with these link-layer protocols. For the following experiments, all four protocols PACE, ACE, HARQ, IEEE802.11 ARQ are implemented with OMNET++ network simulator [19]. We use an Adaptive LDPC (A-LDPC) codes [18] for channel coding operations in PACE and ACE, and Reed-Solomon codes [17] for HARQ[2]

A. Throughput-Delay Tradeoff

The throughput-delay tradeoff suggests that a higher throughput can be achieved with a higher tolerable delay. Consequently, applications with time sensitive delays (realtime delay constraints) suffer from low throughput. In this section, we measure the cost of this tradeoff on the link-layer protocol performance. We define the throughput-delay cost $\zeta(t)$ as follows:

$$\zeta(t) = 1 - \theta(t)\varsigma(t), \quad (23)$$

where the $\theta(t)$ is the throughput cumulative density function (CDF), measuring the fraction of data bits, and $\varsigma(t)$ is the delay CDF, measuring the fraction of packets that are delivered *successfully* to a higher layer by the time t. Notice that the throughput-delay cost function $\zeta(t)$ approaches zero if and only if both $\theta(t)$ and $\varsigma(t)$ approach one at time t.

Consider a packet arrives at time t_0 and has not decoded by time $t \geq t_0$, then its "delay" at time t is by definition $t_n = t - t_0$. In Fig. 4, we show the throughput-delay cost $\zeta(t_n)$ for each protocol with respect to the packet delay t_n over six different wireless channel conditions. Specifically, in Fig. 4(a), where the channel average BER is very low (0.001), we observe that the cost reduces dramatically for the packet delay greater than one. This is so since the likelihood of packet error over this channel is very low. Consequently, most of the packets are received without errors and passed up to the higher layer immediately. However, as the channel BER increases, the likelihood of receiving errornous packets increases. Accordingly, IEEE802.11 ARQ performs retransmissions

[2]It is important to note that HARQ protocols use hard decision algorithms. Reed-Solomon codes are known to be Maximum Distance Separable (MDS) codes and therefore used in HARQ protocols.

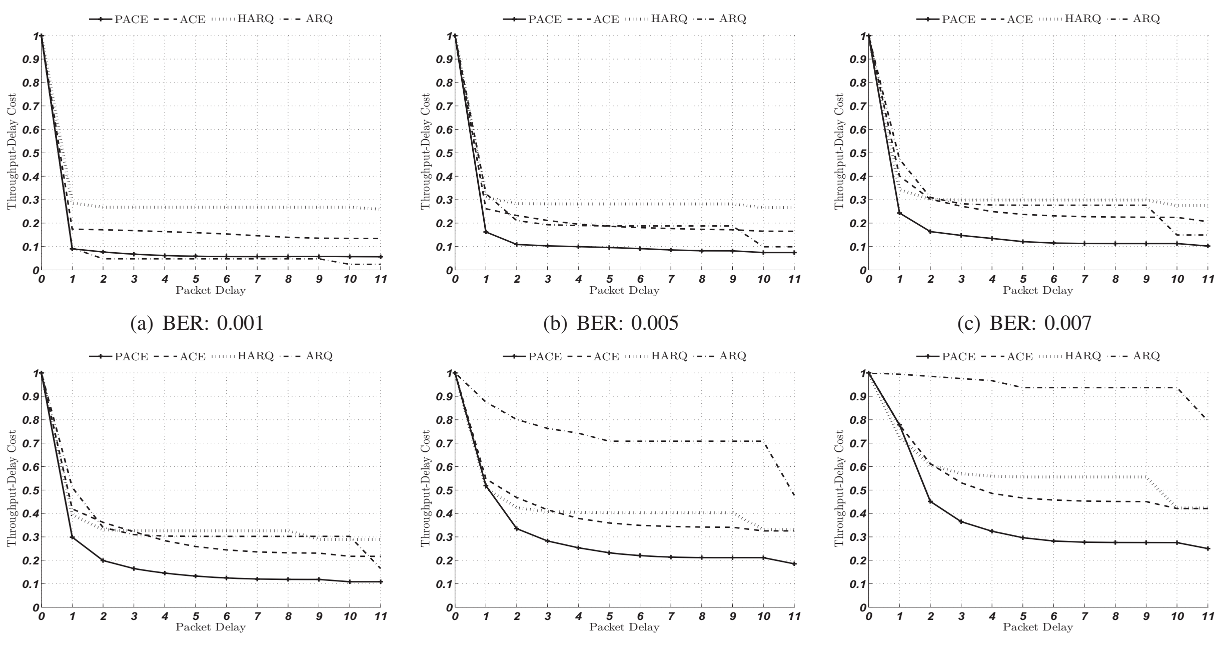

(a) BER: 0.001 (b) BER: 0.005 (c) BER: 0.007

(d) BER: 0.009 (e) BER: 0.018 (f) BER: 0.020

Fig. 4. The variation in throughput-delay cost with respect to the packet delay over different channel traces.

to deliver an error-free packet. This in turn will result in the consumption of channel bandwidth and longer packet delays. Consequently, we observe that the throughput-delay cost for IEEE802.11 ARQ does not reduce significantly as the channel BER increases. For instance, the cost of IEEE802.11 ARQ hovers around 0.7 over the channel with BER 0.018. On the other hand, unlike HARQ, PACE and ACE employ adaptive parity allocation based on the channel condition. Accordingly, we observe that the cost function of these protocols is always lower than HARQ protocol regardless of channel condition. However, for the channel with low BER, where the packet prioritization has no significant impact, we observe that PACE performs better than ACE. We observe this because PACE selects an optimal code to maximize channel bandwidth utilization. In addition, for the channels with higher BER value, PACE still outperforms other protocols since it employs packet prioritization. For instance, the PACE cost reduces below the 0.3 point for packet delays greater than two while ACE, HARQ, and IEEE802.11 ARQ have respective costs of more than 0.4, 0.5 and 0.9. Overall, the PACE protocol gains $10\% - 40\%$ reduction in throughput-delay cost.

B. Realtime and Non-Realtime Application Performance

In this section, we evaluate the performances of a *realtime* video and a *non-realtime* TCP applications in conjunction with PACE, ACE, HARQ and IEEE802.11 ARQ protocols at the link-layer. Fig. 5 illustrates the simulation setup of this section. Specifically, a TCP application sender is sitting at the wired section of the network and transmitting the TCP packets to the wireless receiver. At the same time, a realtime video sender is also transmitting video packets. The TCP and video traffic both are redirected to the receiver by the access point (AP). Using OMNET++ `INET framework`, we implemented this simulation setup for each link-layer protocol. Specifically, for the TCP application sender, we use the `TCPGenericCliAppBase` module to simulate a generic TCP application at the sender and receiver. We evaluate the average throughput of TCP packets. The average throughput measures the fraction of channel capacity that is utilized for a transmission of TCP packets. Further, for the realtime video application, we use `H.264/AVC JM14.0` codec [20] to serve as video encoder/decoder. The realtime video sender encodes *Stefan CIF 30fps* sequence and transmits it to the receiver at 300Kbps video rate. The decoder receives the video packets and decodes them if and only if the video packets arrive before the realtime deadline. Hence, those video packets that miss the deadline are unusable for video decoding. This leads to degradation in video quality as measured by Y-PSNR. Y-PSNR is a function of the mean square error (MSE) between the values of the original and decoded Y frame pixels:

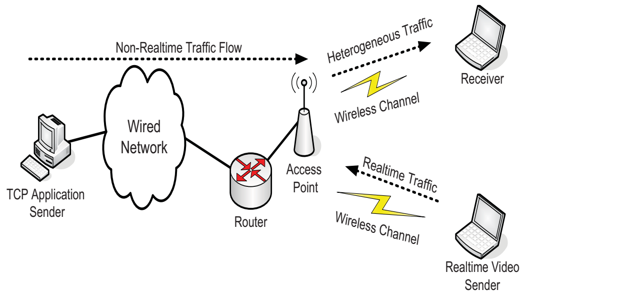

Fig. 5. Simulation setup where heterogeneous traffic is generated by non-realtime TCP and realtime video flows.

$$Y_{PSNR} = 10log_{10}\left[\frac{255^2}{||\mathbf{Y}_{org} - \mathbf{Y}_{dec}||_2^2}\right]. \qquad (24)$$

We repeat this simulation to evaluate the average throughput and PSNR values over 41 channel traces. Therefore, a total of 164 simulations were conducted for this section.

Fig. 6(a) shows the average throughput of the TCP packets over various channel conditions. In this figure the solid line is the channel capacity. The channel capacity gives an upper bound on the average reliable information that can be transmitted over the channel. We observe that for a very low channel BER, IEEE802.11 ARQ achieves a higher throughput than other protocols. This is so since the channel is almost error-free and IEEE802.11 ARQ uses the channel to transmit only data bits. Consequently, its throughput is near channel capacity. On the other hand, PACE and ACE protocols achieve higher throughput than HARQ due the efficacy of adaptive parity allocation. Meanwhile, as the channel BER increases slightly, the performance of IEEE802.11 ARQ decays significantly. The ACE and HARQ protocols manage to perform relatively better than IEEE802.11 ARQ protocol but still their performances are noticeably below the channel capacity. The PACE protocol, however, achieves the average throughput within a maximum of 0.1 distance of the channel capacity. Overall, PACE achieves $20\% - 60\%$ throughput improvement over the IEEE802.11 ARQ and HARQ protocols. In addition, the PACE protocol increases the performance of ACE by 10% regardless of channel condition. This performance gain clearly illustrates the impact of code selection and the decoding scheduling policy of the PACE protocol.

Fig 6(b) suggests that the average Y-PSNR experiences a similar trend. For low BER values, the PSNR value is high and close to the ideal video quality (here $33dB$). However, the PSNR value for IEEE802.11 ARQ and HARQ degrades for channels with BER more than 0.01. The PACE protocol manages to achieve significantly better video quality regardless of channel condition. For instance, the PSNR value is around $31dB$ under PACE while ACE, HARQ, and IEEE802.11 ARQ achieve $28dB$, $27dB$, and $25dB$ over the channel with BER 0.007. Overall PACE achieves $2-10dB$ PSNR gain with respect to the IEEE802.11 ARQ and HARQ protocols. Further, it improves the ACE performance by $1 - 3dB$.

VI. Conclusion

In this paper, we introduced Prioritized Automatic Code Embedding (PACE) protocol which takes into consideration the stability, reliability, and delay constraints in wireless link-layer communication. We developed a LDPC decoding model to capture the decoding process of link-layer traffic and the PACE Buffer model to describe link-layer buffer as a multiclass priority queuing system. Using these models, we determined the optimal code selection for parity allocation and dynamic decoder scheduling for heterogeneous link-layer traffic. We showed experimentally that PACE significantly outperforms IEEE802.11 and HARQ protocols and improves the performance of ACE over various wireless channel conditions.

Appendix

(Proof of Lemma 1): Equation (1) can be simplified significantly with following approximations:

$$\begin{aligned}
\epsilon_i^{(m)} &\approx \epsilon_i^{(0)} - \epsilon_i^{(0)}\left[\frac{1+1-(d_c-1)2\epsilon_i^{(m-1)}}{2}\right]^{d_v-1} \\
&+ (1-\epsilon_i^{(0)})\left[\frac{1+1+(d_c-1)2\epsilon_i^{(m-1)}}{2}\right]^{d_v-1}. \\
&= \epsilon_i^{(0)} - \epsilon_i^{(0)}\left[1-(d_c-1)\epsilon_i^{(m-1)}\right]^{d_v-1} \\
&+ (1-\epsilon_i^{(0)})\left[1+(d_c-1)\epsilon_i^{(m-1)}\right]^{d_v-1}. \\
&\approx \epsilon_i^{(0)} - \epsilon_i^{(0)}\left[1-(d_c-1)\epsilon_i^{(m-1)}\right]^{d_v-1} \\
&= \epsilon_i^{(0)} - \epsilon_i^{(0)}\left[1-(d_v-1)(d_c-1)\epsilon_i^{(m-1)}\right] \\
&= \epsilon_i^{(0)}(d_v-1)(d_c-1)\epsilon_i^{(m-1)} = \xi\epsilon_i^{(m-1)},
\end{aligned}$$

where $\xi = \epsilon_i^{(0)}(d_v-1)(d_c-1)$. By taking a unilateral Z-transform, we have,

$$z\Upsilon_i(z) - \epsilon_i^{(0)} = \xi\Upsilon_i(z) \rightarrow \Upsilon_i(z) = \frac{z^{-1}\epsilon_i^{(0)}}{1-z^{-1}} \tag{25}$$

Now, the inverse Z-transform $u[.]$ gives us the follows:

$$\epsilon_i^{(m)} = \epsilon_i^{(0)}\xi^{-1}u[m] = \epsilon_i^{0}\left[\epsilon_i^{0}(d_v-1)(d_c-1)\right]^{m-1}. \tag{26}$$

This completes the proof. ■

(Proof of Lemma 2): Note that this proof was first presented in [1], and repeated in here to enable coherent exposition. To find the optimal code embedding rate that ensures reliability and stability jointly, we follow a two step proof. First we determine an upper bound on code embedding rate for reliability. Then, we find a lower bound on code embedding rate for stability. The obtained bounds lead to the proof of the Lemma. Based on the reliability analysis in [1], the following optimization problem,

$$\begin{aligned}
&\max k_i \quad \text{subject to:} \\
&k_i\epsilon_i + x_i(\epsilon_i - \alpha) \leq 0 \text{ and } k_i + x_i \leq n_i.
\end{aligned} \tag{27}$$

helps us find an upper bound on the operational code embedding rate that ensures reliability. This optimization problem is a convex problem with the following Lagrangian function

$$\begin{aligned}
L_i(k_i,\lambda_1,\lambda_2) = k_i &+ \lambda_1\left(k_i\epsilon_i + x_i(\epsilon_i-\alpha)\right) \\
&+ \lambda_2\left(k_i + x_i - n_i\right). \ \lambda_1,\lambda_2 > 0
\end{aligned} \tag{28}$$

Since the primal problem is convex, the Karush-Kuhn-Tucker (KKT) conditions are sufficient for the points to be primal and dual optimal (zero duality gap). KKT conditions suggest that based on complimentary slackness property for strong duality, we have

$$\lambda_1\left(k_i^*\epsilon_i + x_i^*(\epsilon_i-\alpha)\right) = 0, \tag{29}$$

$$\lambda_2\left(n_i - k_i^* + x_i^*\right) = 0, \tag{30}$$

where k_i^* and x_i^* are the optimal transmitted amount of data and parity symbols. On the other hand, with the

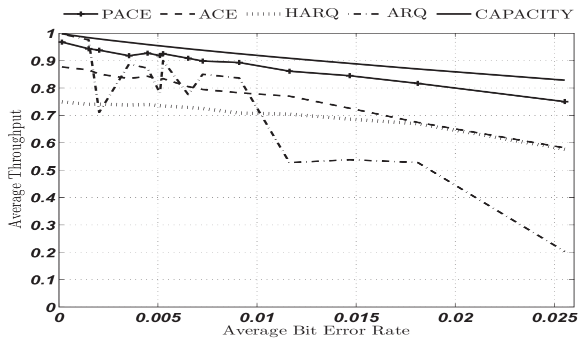

(a) Throughput

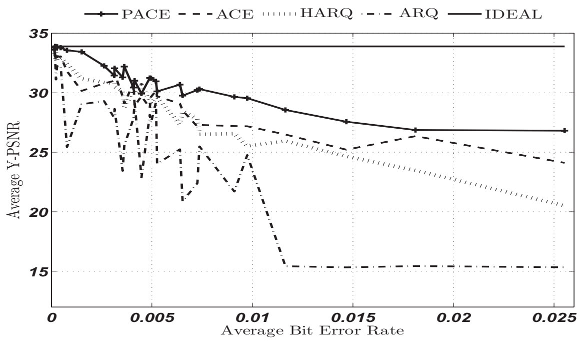

(b) PSNR

Fig. 6. The performances of non-realtime and realtime applications in terms of throughput and video quality.

channel in state S_i, and maximum network utilization of n_i symbols, the amount of transmitted data symbols is bounded above by $k_i = |C_i|R_i \leq k_i^*$, where R_i is a channel coding rate. By substituting $k_i^* = n_iR_i^*, x_i^* = n_i(1 - R_i^*)$ and solve the above equations for R_i^*, we have

$$R_i \leq R_i^* = 1 - \frac{\epsilon_i}{\alpha}. \tag{31}$$

To guarantee the stability condition the buffer has to be always non-empty and at the same time should not overflow. To ensure that the buffer is always non-empty, the buffer length limiting probability distribution should not carry any weight at the value zero (i.e,$F(0, j) = 0, j = 1, 2$). The analysis in [1] shows that the link-layer buffer has the following limiting distributions

$$F(b, 1) = \beta_i(1 - e^{\lambda b}) \tag{32}$$

$$F(b, 2) = \omega_i - \frac{\beta_i(k_i - c)}{c} e^{\lambda b}, \tag{33}$$

where $\lambda = \frac{\beta_i}{c} - \frac{\omega_i}{k_i - c}$. By substituting $b = 0$ in equations (32)(33) we have $F(0, 1) = 0 \quad F(0, 2) = \omega_i - \frac{\beta_i(k_i-c)}{c}$. The steady state probability of the buffer at length zero is always zero when the decoding is successful at the link layer (e.g., $Z(t) = 1$). To ensure that the buffer is non-empty when the link layer fails to decode new data, the following equality has to be satisfied

$$\omega_i = \frac{k_i - c}{k_i}. \tag{34}$$

To avoid buffer overflow, the expected number of data symbols injected into the buffer when the channel is in state S_i. Since the buffer has finite capacity, the following condition has to be satisfied to prevent buffer overflow

$$k_i\omega_i \leq c. \tag{35}$$

where

$$\omega_i = Pr(\text{Successful Decoding in } \tau_i) = F_{E_i}(\alpha x_i). \tag{36}$$

By using equations (36) and (35), we obtain $F_{E_i}(\alpha x_i) = 1 - \frac{c}{k_i} \leq \frac{1}{2}$. Therefore, $x_i \leq \frac{F_{E_i}^{-1}(0.5)}{\alpha} = \frac{\lambda_{E_i}}{\alpha} = \frac{|C_i|\epsilon_i}{\alpha}$. Correspondingly, by substituting $x_i = |C_i|(1 - R_i)$, the lower bound of code embedding rate is

$$R_i \geq 1 - \frac{\epsilon_i}{\alpha}. \tag{37}$$

Equations (31) and (37) suggest that an optimal solution for code embedding rate that ensures reliability and stability conditions is a unique solution:

$$R_i^* = 1 - \frac{\epsilon_i}{\alpha}. \quad \epsilon_i \ll \alpha \tag{38}$$

■

REFERENCES

[1] S. Soltani, K. Misra, and H. Radha, "On Link-Layer Reliability and Stability for Wireless Communication," ACM MOBICOM, 2008.

[2] X. Liu, E. K. P. Chong, and N. B. Shroff, "Opportunistic transmission scheduling with resource-sharing constraints in wireless networks," IEEE J. Sel. Areas Commun., vol. 19, no. 10, pp. 20532064, Oct. 2001.

[3] M. Andrews, K. Kumaran, K. Ramanan, A. L. Stolyar, R. Vijayakumar, and P. Whiting, "Providing quality of service over a shared wireless link," IEEE Commun. Mag., vol. 39, no. 2, pp. 150154, Feb. 2001.

[4] P. Bhagwat, P. Bhattacharya, A. Krishna, and S. K. Tripathi, "Enhancing throughput over wireless LANs using channel state dependent packet scheduling," IEEE INFOCOM 1996.

[5] S. Shakkottai and R. Srikant, "Scheduling real-time traffic with deadlines over a wireless channel," 2002 ACM Wireless Netw. J.

[6] J. Huang, R. A. Berry, and M. L. Honig, "Wireless Scheduling With Hybrid ARQ", IEEE Trans. Wire. Commun. vol. 4, no. 6, 2005.

[7] A. Banerjee, D. Costello, and T. Fuja, "Diversity combining techniques for bandwidth-efficient turbo ARQ systems," in IEEE Int. Symp. Information Theory, Washington, DC, Jun. 2001, p. 213.

[8] D. Chase, "Code-combiningA maximum likelihood decoding approach for combining an arbitrary number of noisy packets," IEEE Trans. Commun., vol. COMM-33, no. 5, pp. 385393, May 1985.

[9] J. Hagenauer, "Rate-compatible punctured convolutional codes and their applications," IEEE Trans. Commun., vol.36, no. 4, Apr. 1988.

[10] M. Mandelbaum, M. Hlynka, and P. H. Brill,"Nonhomogeneous geometric distributions with relations to birth and death processes," Springer journal TOP on Business and Economics, July 2007.

[11] R. G. Gallager, "Low Density Parity Check Codes," Trans. of the IRE Prof. G. Info. Theo., vol. IT-8, January 1962, pp. 21-28.

[12] W. E. Ryan, "An introduction to LDPC codes," August 2003.

[13] E. Plambeck, S. Kumar, and J. M. Harrison, " A Multiclass Queue in Heavy Traffic with Throughput Time Constraints: Asymptotically Optimal Dynamic Controls," Queu. Sys. Springer J. vol. 39, No. 1, 2001.

[14] S. Karande, "A Simple Relationship between Iterations and Error," Private Communication, 2008.

[15] S. M. Ross, "Introduction to Probability Models", Acad. Press. 2003.
[16] S. Boyd and L. Vandenberghe, "Convex Optimization,"Cambridge University Press 2004.
[17] "Reed-Solomon source code", http://www.eccpage.com/
[18] "LDPC Software", http://www.cs.utoronto.ca/radford/ldpc.software.html
[19] OMNeT++ Community, http://www.omnetpp.org.
[20] H.264/AVC Software Coordination http://iphome.hhi.de/suehring/tml/

Sohraab Soltani received the Ph.D. degree from Michigan State University in 2009, the M.S. degree from Michigan State University in 2006, and the B.S. degree (with honors) from Shiraz University in 2002 (all in Computer Science). Currently, he is an Assistant Professor of Computer Science at University of Texas at Tyler (UTT) and the Director of the Stochastic Wireless and Visual Information Laboratory at UTT. His research interest includes wireless communication, wireless networking, stochastic modeling, and channel coding.

Hayder Radha received the Ph.M. and Ph.D. degrees from Columbia University in 1991 and 1993, the M.S. degree from Purdue University in 1986, and the B.S. degree (with honors) from Michigan State University (MSU) in 1984 (all in electrical engineering). Currently, he is a Professor of Electrical and Computer Engineering (ECE) at MSU, the Associate Chair for Research and Graduate Studies of the ECE Department, and the Director of the Wireless and Video Communications Laboratory at MSU. Professor Radha was with Philips Research (1996-2000), where he worked as a Principal Member of Research Staff and then as a Consulting Scientist in the Video Communications Research Department. He became a Philips Research Fellow in 2000. Professor Radha was a Distinguished Member of Technical Staff at Bell Laboratories where he worked between 1986 and 1996 in the areas of digital communications, image processing, and broadband multimedia.

Professor Radha served as Co-Chair and Editor of the ATM and LAN Video Coding Experts Group of the International Telecommunications Union - Telecommunications Section (ITU-T) between 1994-1996. He currently serves on the Editorial Board of IEEE Transactions on Multimedia and the Journal on Advances in Multimedia. He is an elected member of the IEEE Technical Committee on Multimedia Signal Processing and the IEEE Technical Committee on Image and Multidimensional Signal Processing (IMDSP). He also served as a Guest Editor for the special issue on Network-Aware Multimedia Processing and Communications of the IEEE Journal on Selected Topics in Signal Processing. Professor Radha is a recipient of the Bell Labs Distinguished Member of Technical Staff Award, the AT&T Bell Labs Ambassador Award, AT&T Circle of Excellence Award, the MSU College of Engineering Withrow Distinguished Scholar Award for outstanding contributions to engineering, and the Microsoft Research Content and Curriculum Award. He is also a recipient of National Science Foundation (NSF) Theoretical Foundation, Network Systems, and Cyber-Trust awards. His current research areas include wireless communications and networking, sensor networks, network coding, video coding, stochastic modeling of communication networks, and image and video processing. He has more than 100 peer-reviewed papers and 30 US patents in these areas.